Mathematics Notes

Note 61

August 1978

Comparison of Three Techniques for Calculating Poles and Residues from Experimental Data

J. T. Cordaro
University of New Mexico
Albuquerque, New Mexico

Abstract

Three pole and residue calculation techniques are compared by applying the methods to simulated data. Each method works well when the data consist of a damped sinusoid plus noise. But when the data include effects from pulser asynchronism and ground reflection, accurate pole calculation is more difficult. For the methods to produce accurate results under some EMP test conditions, it will be necessary to use incident field data and information about the SEM coupling coefficients and natural modes of the body exposed to EMP.

Section I

Introduction

Several investigators have looked at the problem of calculating poles and residues from experimental data (refs. 1, 2, 3, 4). The common conclusion is that each author's approach gives accurate results when the data consist of damped sinusoids plus noise. Recently, poles and residues were calculated for data from the ATHAMAS pipe test (ref. 5). It was observed that the data recorded under actual EMP test conditions are not simply sums of damped sinusoids. Because of pulser asynchronism and ground reflection, the data contains damped sinusoid responses but delayed by various amounts. These delays introduce a number of poles into the data that can interfere with or prevent the calculation of poles due to the illuminated test body response.

If the delay is due to pulser asynchronism, then the effect is contained in the incident field waveform. In principle, at least, this effect can be unfolded by simply dividing the response Fourier transform by the incident field Fourier transform. (Of course there are practical problems if the latter transform has zeros.) But it is worth noticing that the ground reflection problem cannot be handled so easily.

To show this, consider the case of a delta function excitation on a finite size, perfectly conducting body in free space. The Laplace transformed surface current can be expressed (ref. 6) as

$$\bar{Y}(\bar{r},s) = \sum_k \eta_k(\bar{I}_1,s_k)\,\bar{\nu}_k(\bar{r})(s - s_k)^{-1} \qquad (1)$$

where

$\eta_k(\bar{I}_1,s_k)$ is the coupling coefficient

$\bar{\nu}_k(\bar{r})$ is the natural mode vector

and

s_k is a natural frequency of the body

If the total incident field consists of direct and reflected components, then the total response will be the superposition of the responses from each field component

$$\bar{Y}(\bar{r},s) = \sum_k \left[\eta_k(\bar{l}_1,s_k) + e^{-sD}\, K(s)\, \eta_k(\bar{l}_2,\, s_k)\right] \bar{\nu}_k(\bar{r})(s - s_k)^{-1} \qquad (2)$$

where

$\eta_k(\bar{l}_2,s_k)$ is the coupling coefficient due to the reflected wave

K(s) is the reflection coefficient

and

D is the time delay between the direct and reflected waves

The constant D can be computed from geometry, and it may be possible to measure K(s). But the coupling coefficients are unknown except as factors in $\bar{Y}(\bar{r},s)$. Because of the time delay D, the time domain response actually consists of damped sinusoids starting at t = 0 plus more damped sinusoids starting at t = D. As will be shown below, this makes the problem of computing the s_k more difficult than if no reflected wave is present.

The author has been experimenting with three different pole extraction techniques. This memo contains:

(1) Results on the performance of each technique when random noise is present, and

(2) Some initial results on how delays in the data affect each technique.

Section II

Damped Sinusoids with Noise

The three techniques are Prony's method (refs. 1, 4), the interative premultiply method (ref. 8), and the prefilter method (refs. 7, 9, 10). These methods are discussed in the references and will be described briefly here.

Originally, Prony's method was used to fit exponential functions to data. Several numerical analysis texts (see ref. 11, for example) have examples showing that the technique is extremely sensitive to inaccuracies in the data. More recent work (refs. 1, 4) has shown that by "overfitting" the data, good results can be obtained. For example, if a signal consisting of a single damped sinusoid (two exponentials) plus noise is analyzed, it might be necessary to fit a system of order 15. The calculations involve solving 15 simultaneous linear equations and factoring a polynomial of order 15. Details of the calculations are left to the references.

The iterative premultiply method (ref. 8) attempts to minimize the mean squared error between the data and a sum of exponentials. A direct approach to this minimization problem requires the solution of a set of coupled non-linear algebraic equations. The premultiply method attempts to find the solution by an interative technique. For a signal consisting of a single damped sinusoid plus noise the method fits a system of order 2 and factors a second degree polynomial. But the iterative procedure requires repeatedly solving linear equations approximately of order 40. The overall computation is about five times that required by Prony's method.

The prefilter method (refs. 9, 10) involves filtering the data with an adaptive filter and solving linear equations. It requires the specification of a known forcing function as the input to a linear system whose output is the measured data. For

the simulation study discussed below the forcing function was taken as a delta function at t = 0. But for some applications that will be discussed later, the incident field function is a more appropriate forcing function. If the data consists of M damped sinusoids plus noise, the method requires solving 4M linear equations, factoring an Mth order polynomial, and repeatedly filtering the data. The method requires about 1/3 the time required by Prony's method.

Each method was tested on the signal

$$y(nT) = \exp(-nT)\sin(3.14nT),\ n = 0,1,\ldots,N-1 \qquad (3)$$

where

T = sampling interval

N = number of data points

To simulate the effect of measurement noise, a sequence of pseudo-random numbers was generated and added to the y(nT). The random numbers were independent, uniformly distributed with mean zero and standard deviation a given percent of the peak value of y(nT).

The three methods were tested with several different noise levels. For a given noise level, a test consisted of generating fifty different simulated data sequences. The choice of fifty as the number of trials was arbitrary, and the random numbers were different for each sequence. Then poles were calculated for each of the fifty data sequences. Finally, the average and variance of the poles were calculated.

The results are displayed in tables 1 and 2. The premultiply and prefilter methods give identical results in this case. Based on these two tables, it would appear that the two iterative methods produce more accurate results. This is quite noticeable at the higher noise levels. A random noise level of about 1% is what can be expected from normal EMP test data (see ref. 12, for example). At this low level of noise, each of the three methods

Table 1. Pole mean and variance for 50 trials vs percent noise. Signal poles were $-1 \pm j3.14$ and N = 50, T = .04 on each run. Prony's method using 20 poles total.

Percent Noise	Mean Real Part	Mean Imaginary Part	Real Part Variance	Imaginary Part Variance
1	-1.000	3.140	.168E-3	.110E-3
5	-1.007	3.143	.432E-2	.290E-2
10	-1.034	3.154	.182E-1	.126E-1
15	-1.079	3.173	.441E-1	.313E-1
20	-1.142	3.199	.862E-1	.634E-1

Table 2. Pole mean and variance for 50 trials vs percent noise. Signal poles were $-1 \pm j3.14$ and N = 50, T = .04 on each run. Iterative premultiply method or prefilter method using two poles.

Percent Noise	Mean Real Part	Mean Imaginary Part	Real Part Variance	Imaginary Part Variance
1	-1.000	3.139	.715E-4	.240E-4
5	-1.003	3.136	.183E-2	.600E-3
10	-1.013	3.133	.766E-2	.241E-2
15	-1.029	3.131	.185E-1	.547E-2
20	-1.053	3.131	.364E-1	.985E-2

gives acceptable results. For reference, graphs of some of the functions used in the simulation are shown in Figures 1 through 6. Fourier transform magnitudes are included also. Just to show how well the prefilter method can work with noisy data, another set of 50 trials was made with N = 200, T = .01 and 20% noise. Even with this high noise level, the mean pole location was -1.007±j.3.134 with variances of .612E-2 for the real part and .264E-2 for the imaginary part. These simple examples indicate that for accurate pole calculation, low level random noise is not a problem. Other types of instrumentation error found in EMP test data are discussed in reference 12. These other errors are not considered here.

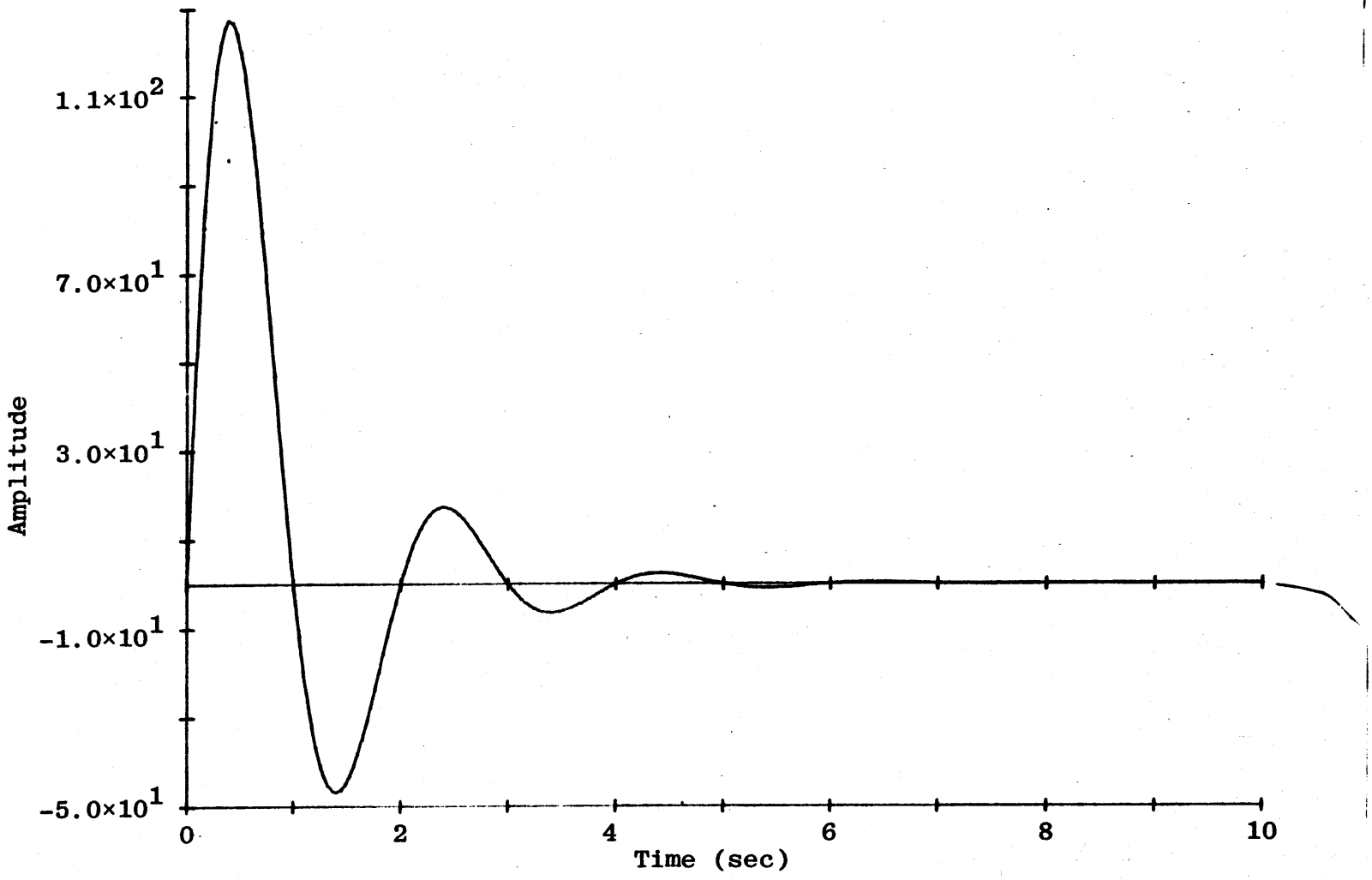

Figure 1. Damped Sinewave Used in Simulation. No Additive Noise

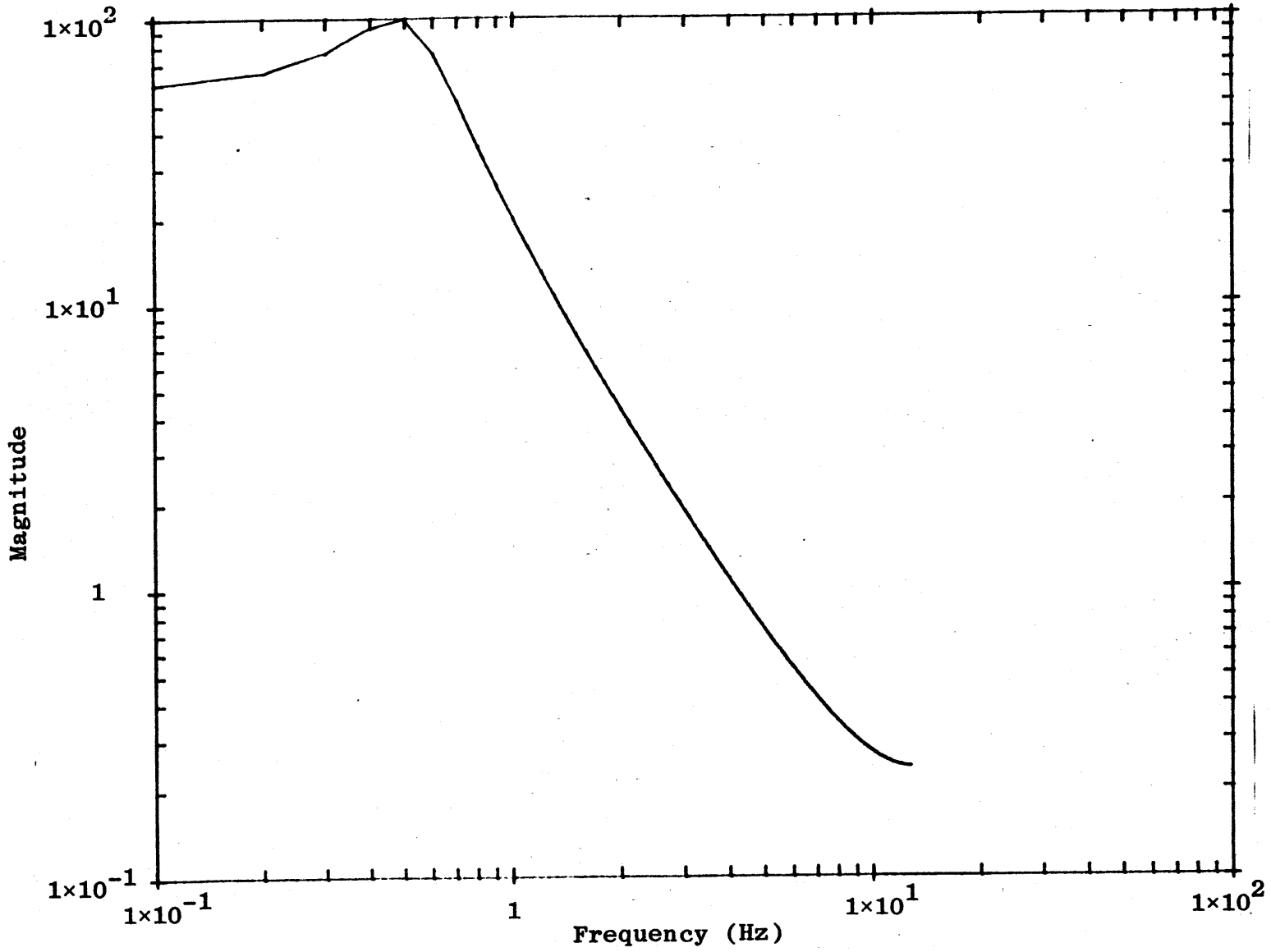

Figure 2. Transform Magnitude of Damped Sinewave Used in Simulation

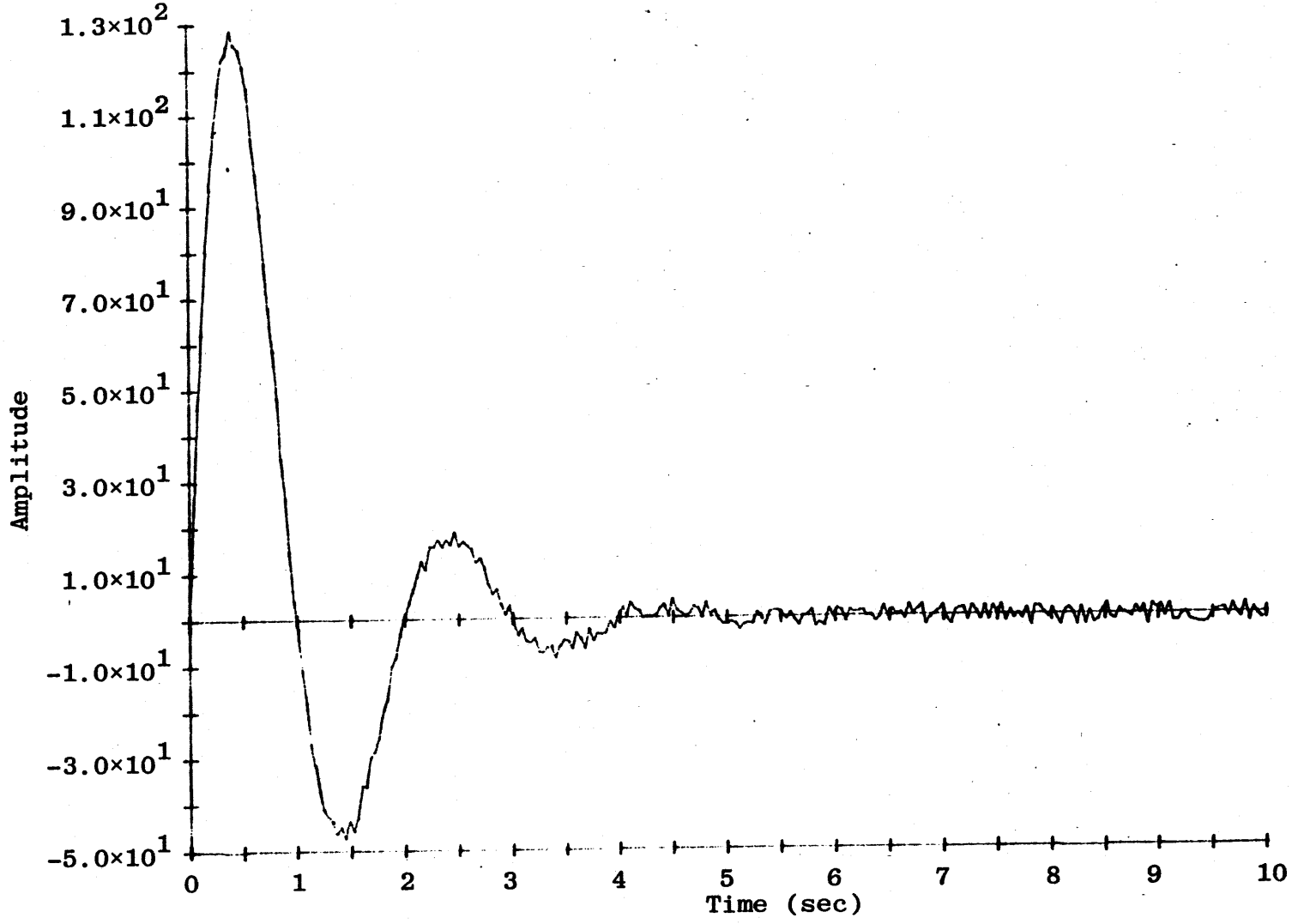

Figure 3. Damped Sinewave with 1% Additive Noise

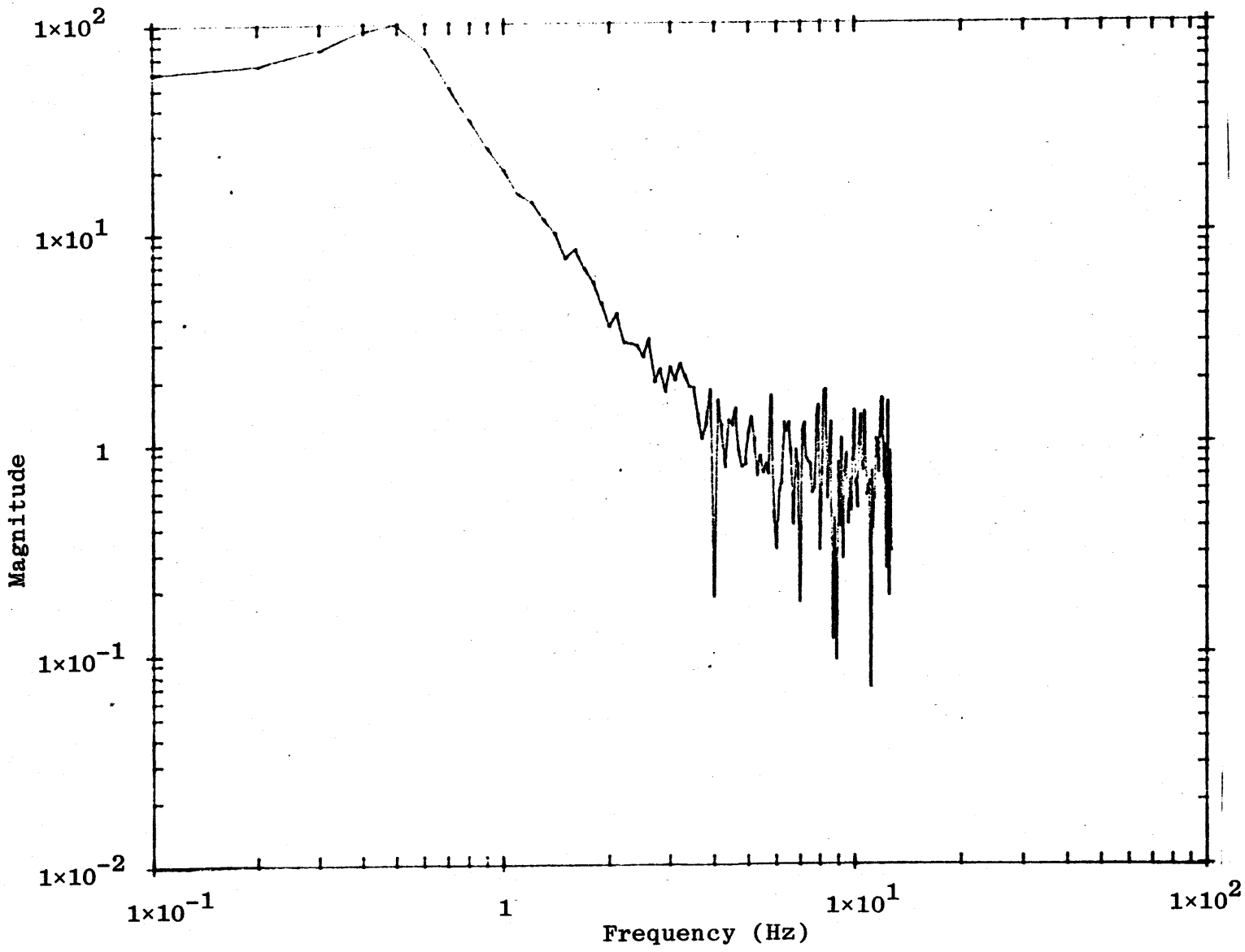

Figure 4. Transform Magnitude of Damped Sinewave with 1% Noise

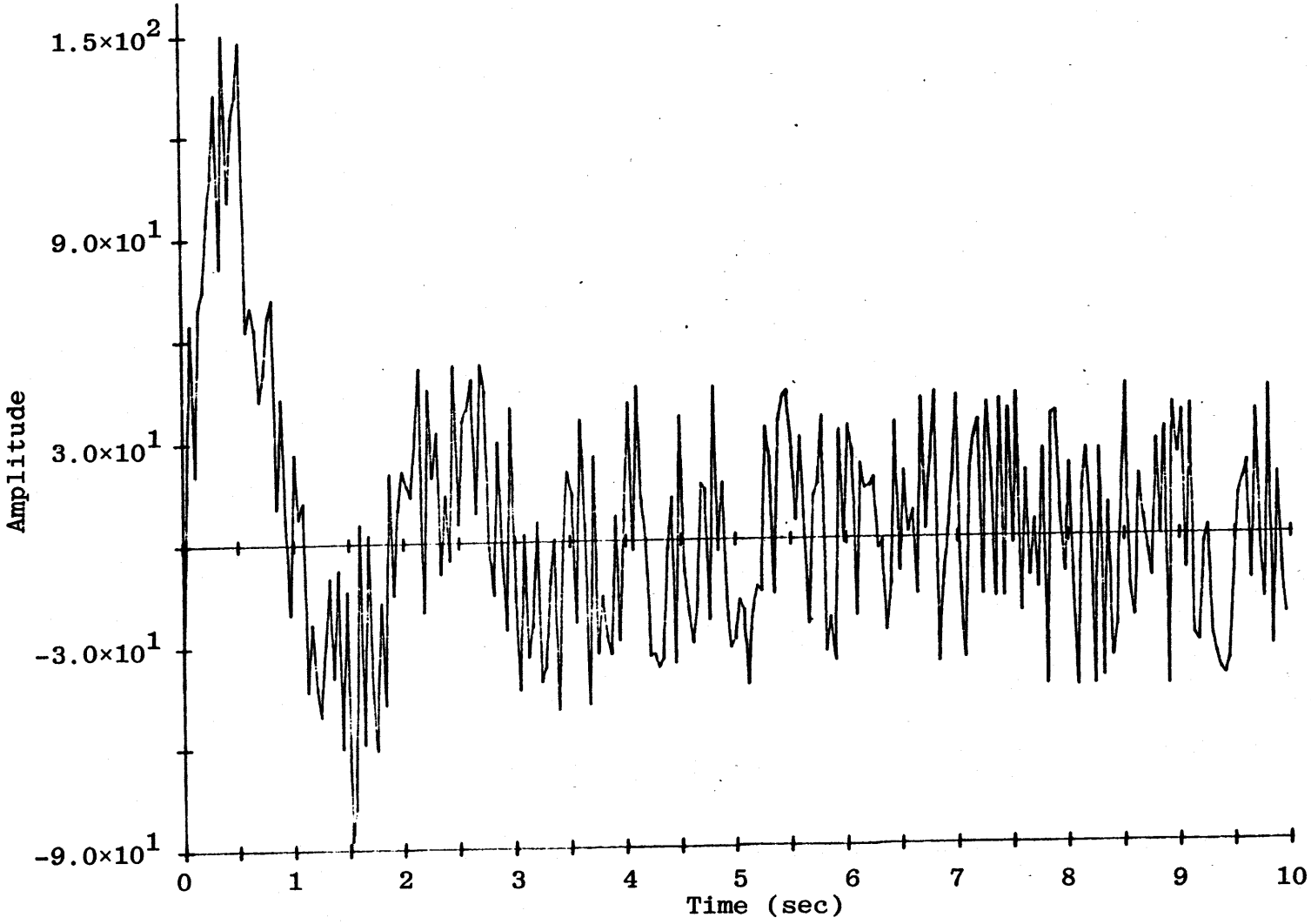

Figure 5. Damped Sinewave with 20% Additive Noise

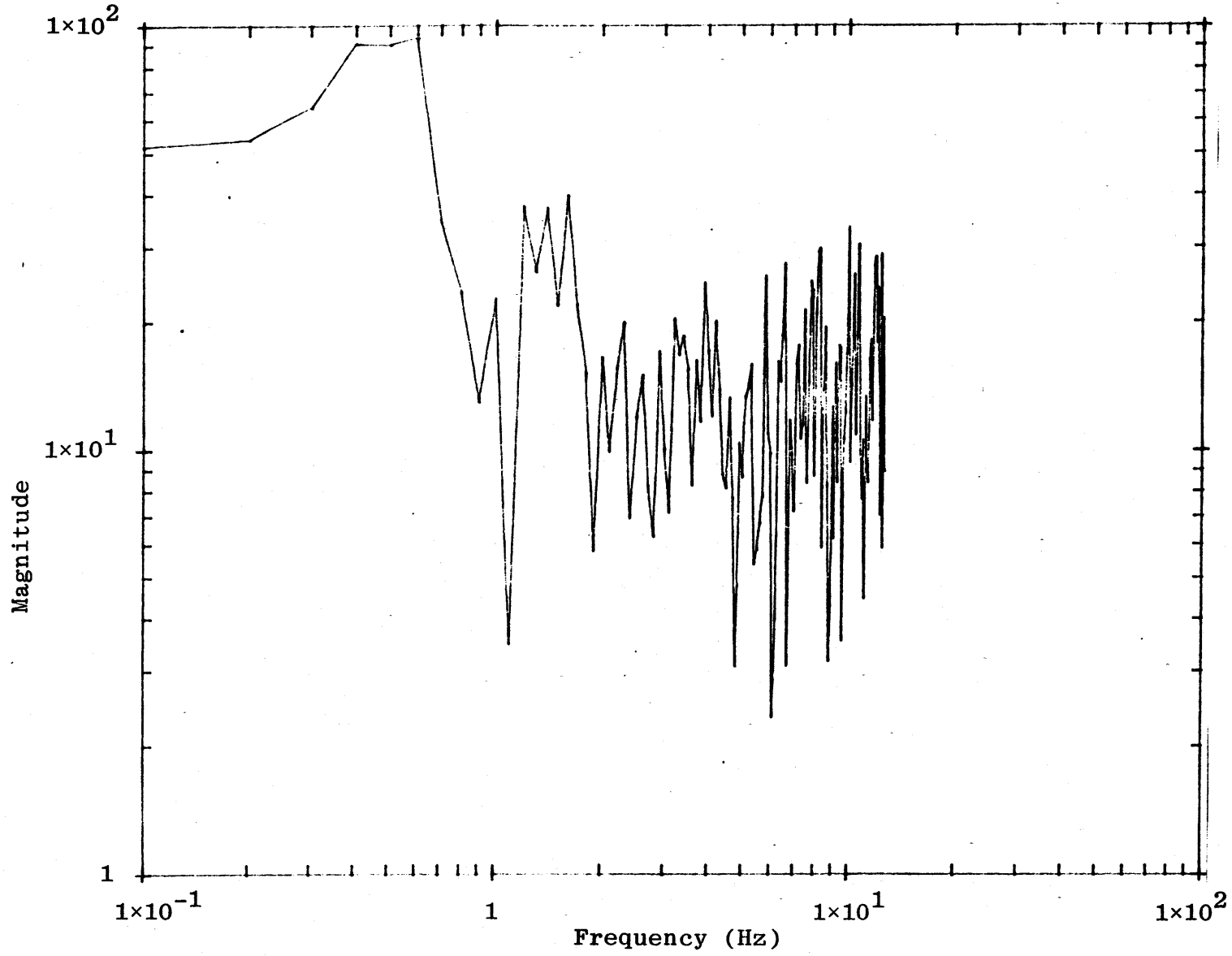

Figure 6. Transform Magnitude, Damped Sinewave with 20% Noise

Section III

Delays

The most serious problem in analyzing test data using any of the three methods is the presence of non-sinusoidal data components. Each method models the observed signal as a sum of complex exponentials plus random noise. If the actual signal is not in this form, then a number of extra poles and residues must be fitted to account for non-sinusoidal signal components. One common source of these components is the pulser used to generate the incident field. Experience has shown that the waveform from the ATHAMAS I simulator cannot be represented by a low order sum of complex exponentials (ref. 5). As a result, the total measured response of a test object at ATHAMAS I consists of damped sinusoids from the object response plus components from the pulser that cannot be represented easily by damped sinusoids.

Another problem comes from the fact that the total incident field at this simulator consists of direct and reflected waves. The starting time of the latter may be delayed by 50 ns or more from the arrival of the direct wave. This delay stretches out the time that the incident field is turned on and generates additional non-sinusoidal components in the measured data. Whether or not these problems interfere with the calculation of object response poles depends on a number of factors. Some of these factors are considered in this section.

The next set of experiments involves the function $(y(t)\ u(t) + y(t - D)\ u(t - D))$ where D is the delay, u(t) is the unit step function, and y(t) is given by equation 3. This sum can simulate the effect of pulser asynchronism for small values of D and the effect of ground bounce for larger values of D.

This simulation is oversimplified. With actual test data, the transform of y(t) would contain both incident field and object poles. Also, for modeling ground reflection, a reflection

coefficient, K(s) $\neq$ 1, should be included. But using a waveform y(t) with only two poles, -1±j3.14, keeps the analysis simple and focuses attention on the effect of changes in D.

In each experiment involving delay, pseudo-random 1% noise was added to the signal. (The required noise standard deviation is a function of D since the peak signal value depends on D.) The results of 50 trials are shown in Table 3.

Table 3. Pole mean and variance for 50 trials vs delay. Signal poles were -1±j3.14 and N = 50, T = .04, 1% noise. Premultiply and Prony's methods.

D	Mean Real Part	Mean Imaginary Part	Real Part Variance	Imaginary Part Variance	Method
.25	-.998	3.136	.568E-3	.801E-3	Premultiply
.5	-.985	3.121	.381E-2	.119E-1	Premultiply
.25	-.997	3.137	.161E-3	.574E-3	Prony
.5	-.995	3.112	.251E-2	.114E-1	Prony

The trials using each method were done with 20 poles. A number of poles in addition to the poles of y(t) are required to fit the extra data structure due to the delay. Time and frequency domain graphs of the signals are given in figures 7 through 10. The mean pole values in table 3 were computed starting the analysis at time = 0. When the starting time for the analysis is changed, these mean pole values change also.

From table 3, it can be seen that the iterative method works about as well as Prony's method. Either technique gives results that are acceptable for small values of D. As D increases, the pole error increases. Figures 8 and 10 help explain why this is so. For small D, the first null in the Fourier transform is far away from the peak in the transform of y(t). But the null moves closer to the peak as D increases. (For a reflection coefficient of +1, nulls lie at odd multiples of 1/2 D.)

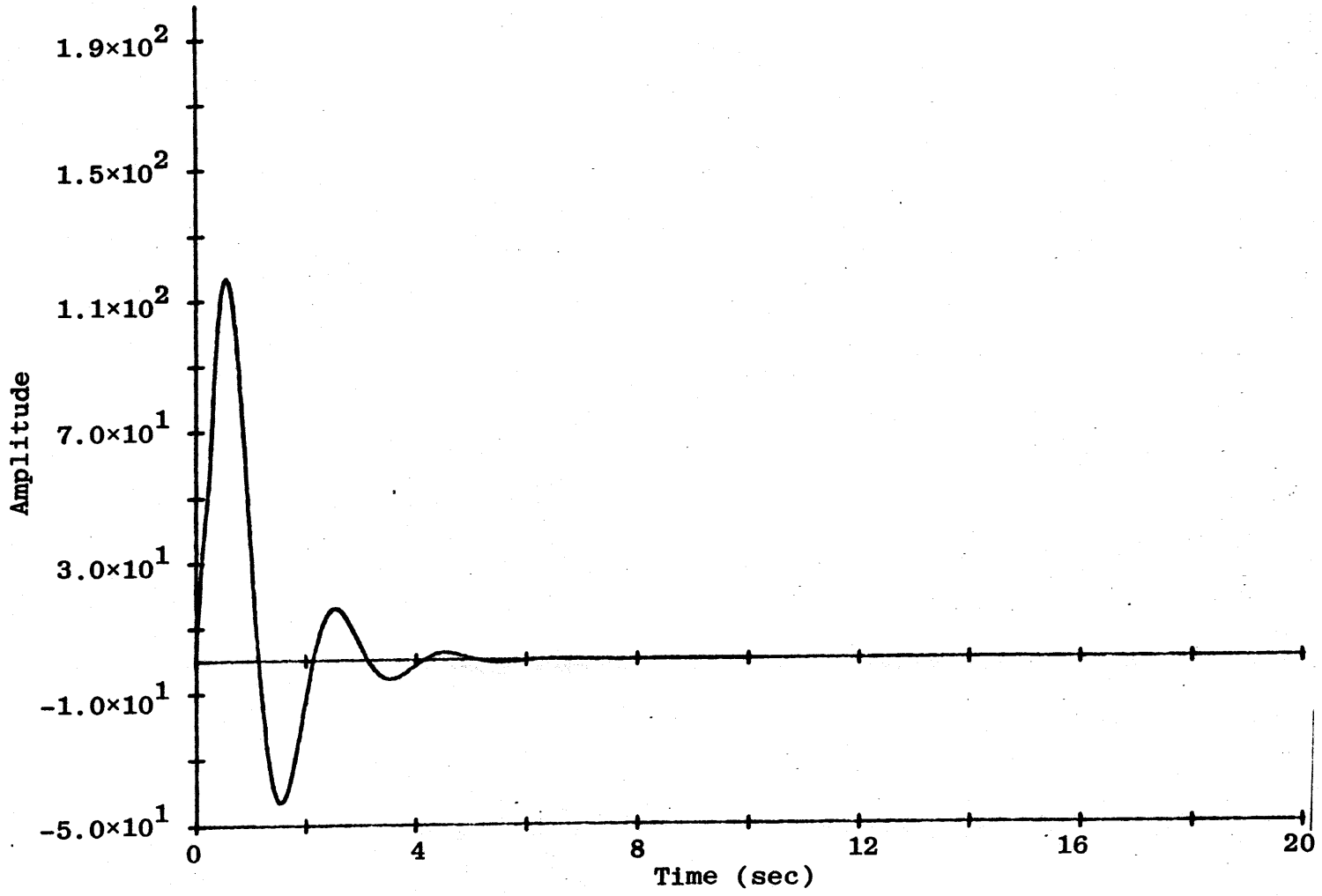

Figure 7. Delayed Damped Sinewaves. D = .25

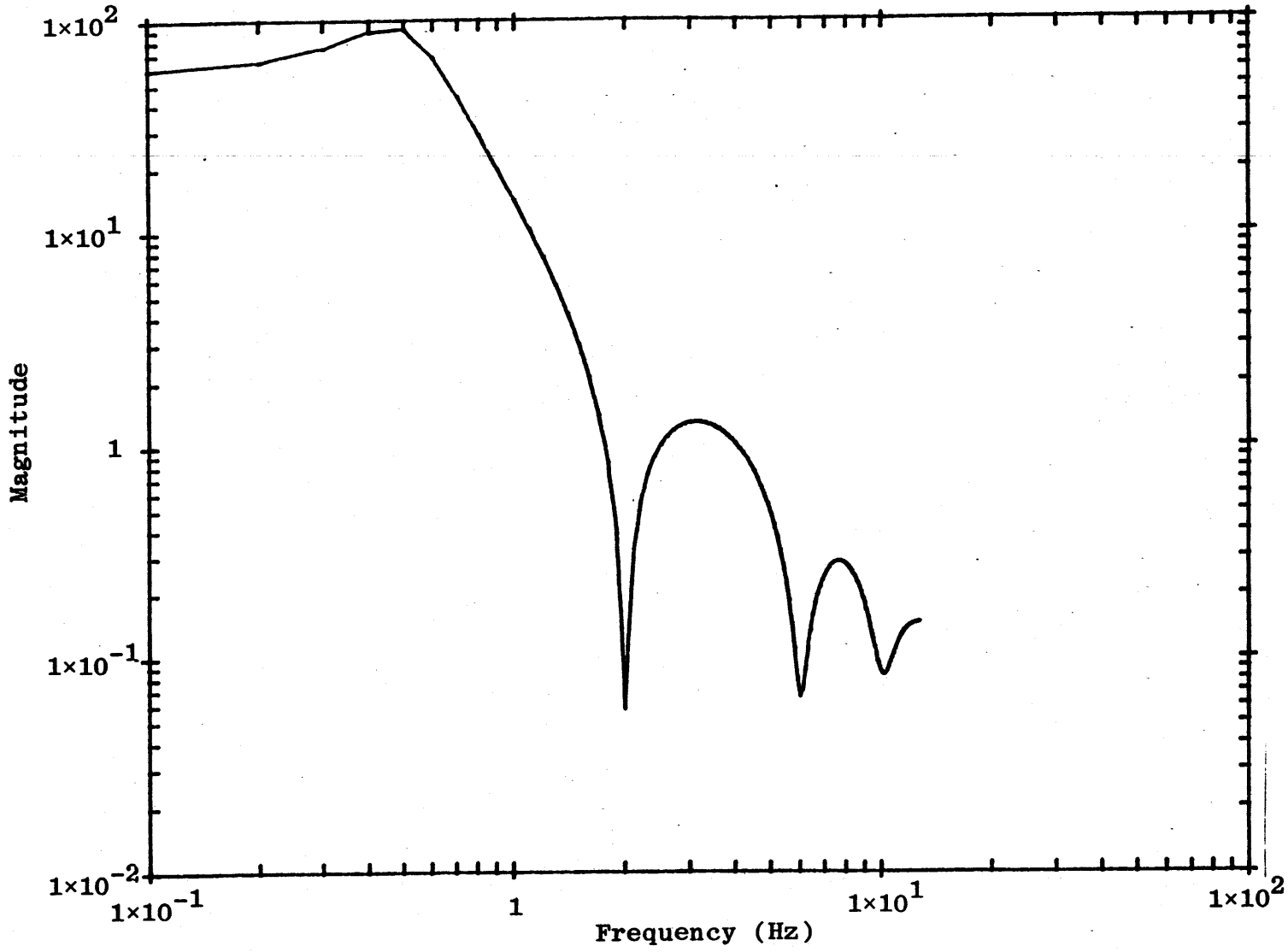

Figure 8. Transform Magnitude, Delayed Damped Sinewaves. D = .25

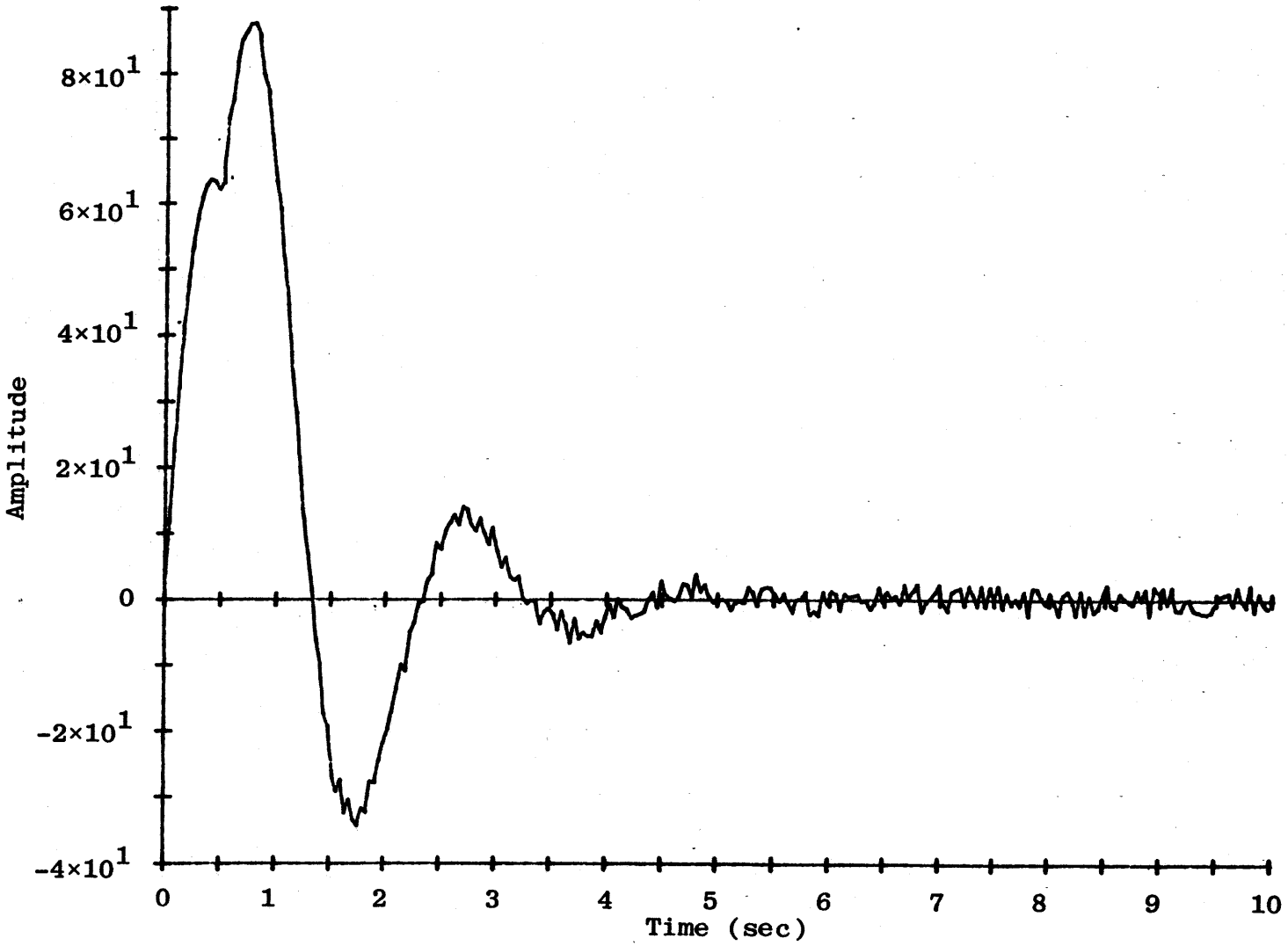

Figure 9. Delayed Damped Sinewaves with 1% Noise. D = .50

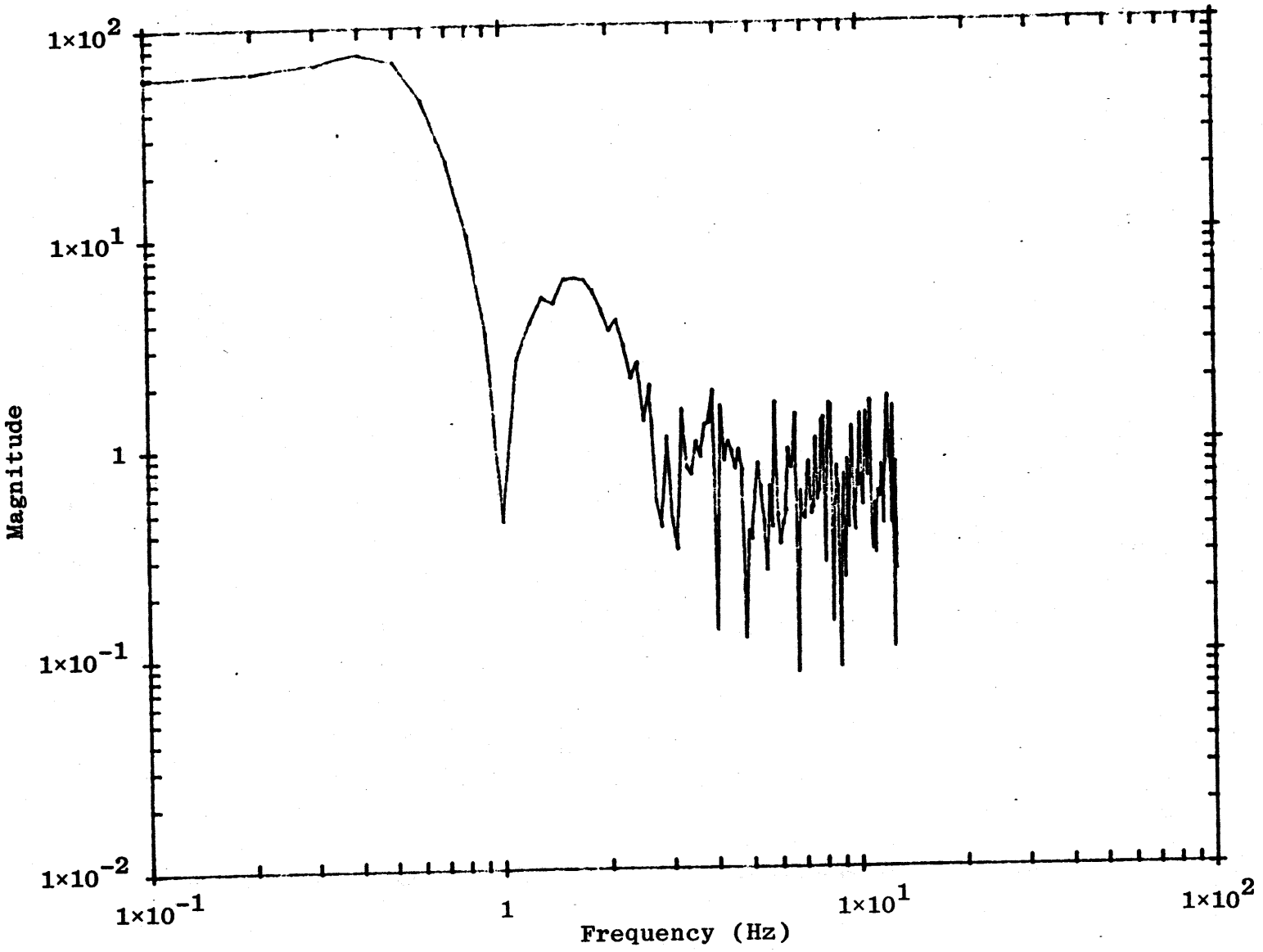

Figure 10. Transform Magnitude, Delayed Damped Sinewaves. D = .50, 1% Noise

It is interesting to see what happens when the first null coincides with the peak of the signal transform. A graph of this case is shown in figure 11 and the corresponding transform in figure 12. Graphs for the 1% noise case are in figures 13 and 14. The poles and residues calculated with Prony's method are shown in table 4 for the noiseless case and in table 5 for the 1% noise case. It is no surprise that the poles of (ynT) do not appear in the tables. The only poles are those corresponding to the peaks in the Fourier transform at even multiples of 1/2 D. (The radian frequencies are even multiples of π.) In this example, it appears that the effect of delay has completely obscured the poles of y(t). However, a little common sense suggests that if the data are analyzed from 0.0 to 1.0, that is before the delayed part of the signal begins, it should be possible to find the poles of y(t). This of course turns out to be true.

Alternatively, if D is known, then the analysis can be started after t = D. If it can be done, this is the best choice. For t > D

$$\begin{aligned} y(t)u(t) + y(t-D)u(t-D) &= \exp(-t)\sin(3.14t) + \exp(-(t-D))\sin 3.14(t-D) \\ &= \exp(-t)(\sin 3.14t + \exp(D)\sin 3.14(t-D)) \\ &= \exp(-t)\, A \sin(3.14t + B) \qquad (4) \end{aligned}$$

for some A and B. So that the waveform for t > D has only the poles of y(t), and no poles due to the delay. This argument generalizes to the case where y(t) is a sum of damped sinusoids.

So there are two extreme cases. If the delay is small enough that the first null is not near the signal peak, then signal poles can be calculated accurately. If the delay is large enough that part of the data can be analyzed without including the turn-on time of the delayed component then object poles can be calculated accurately. Real data can fall into one of these two nice classes. For example, the first null produced by pulser

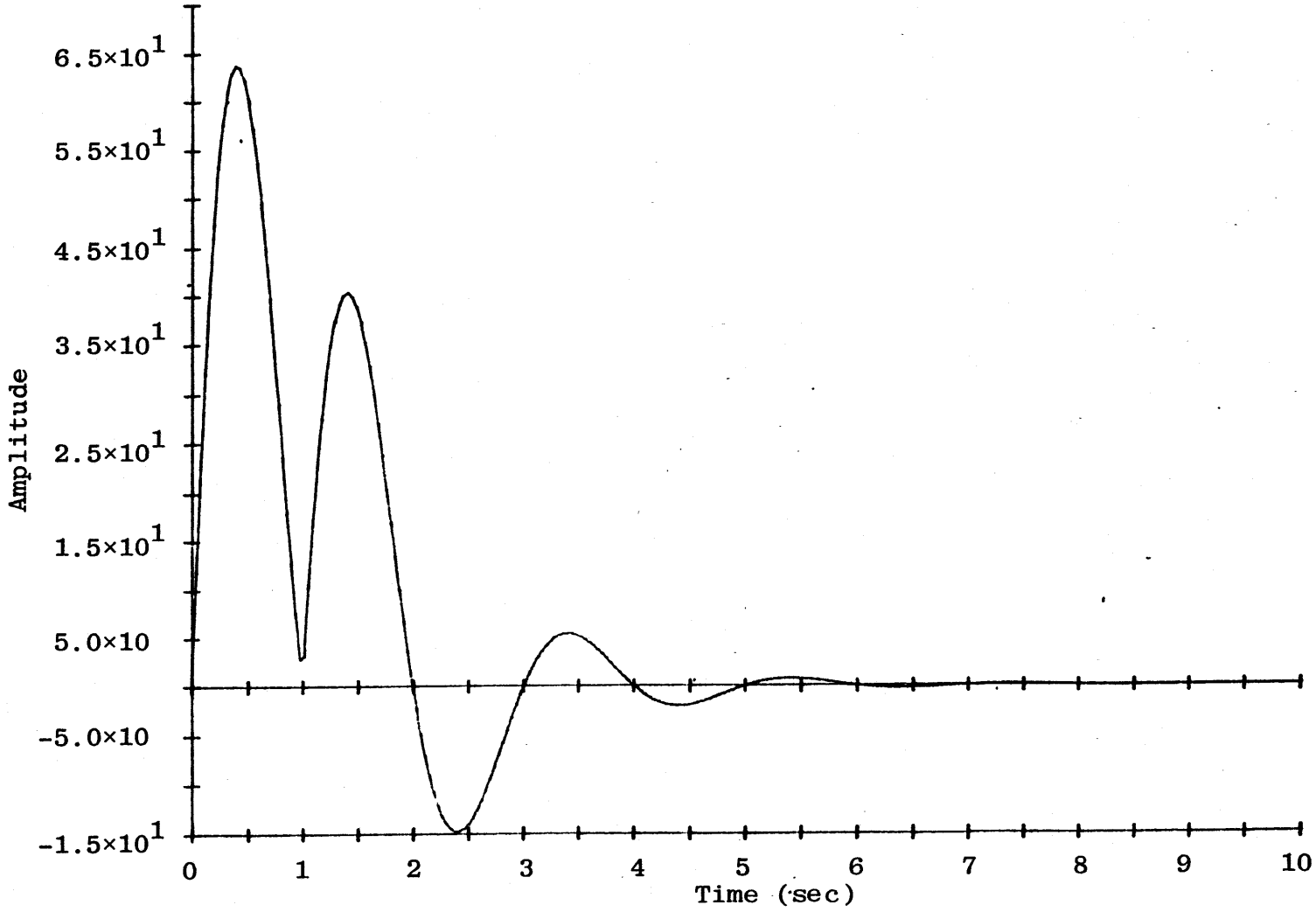

Figure 11. Delayed Damped Sinewaves. D = 1.00

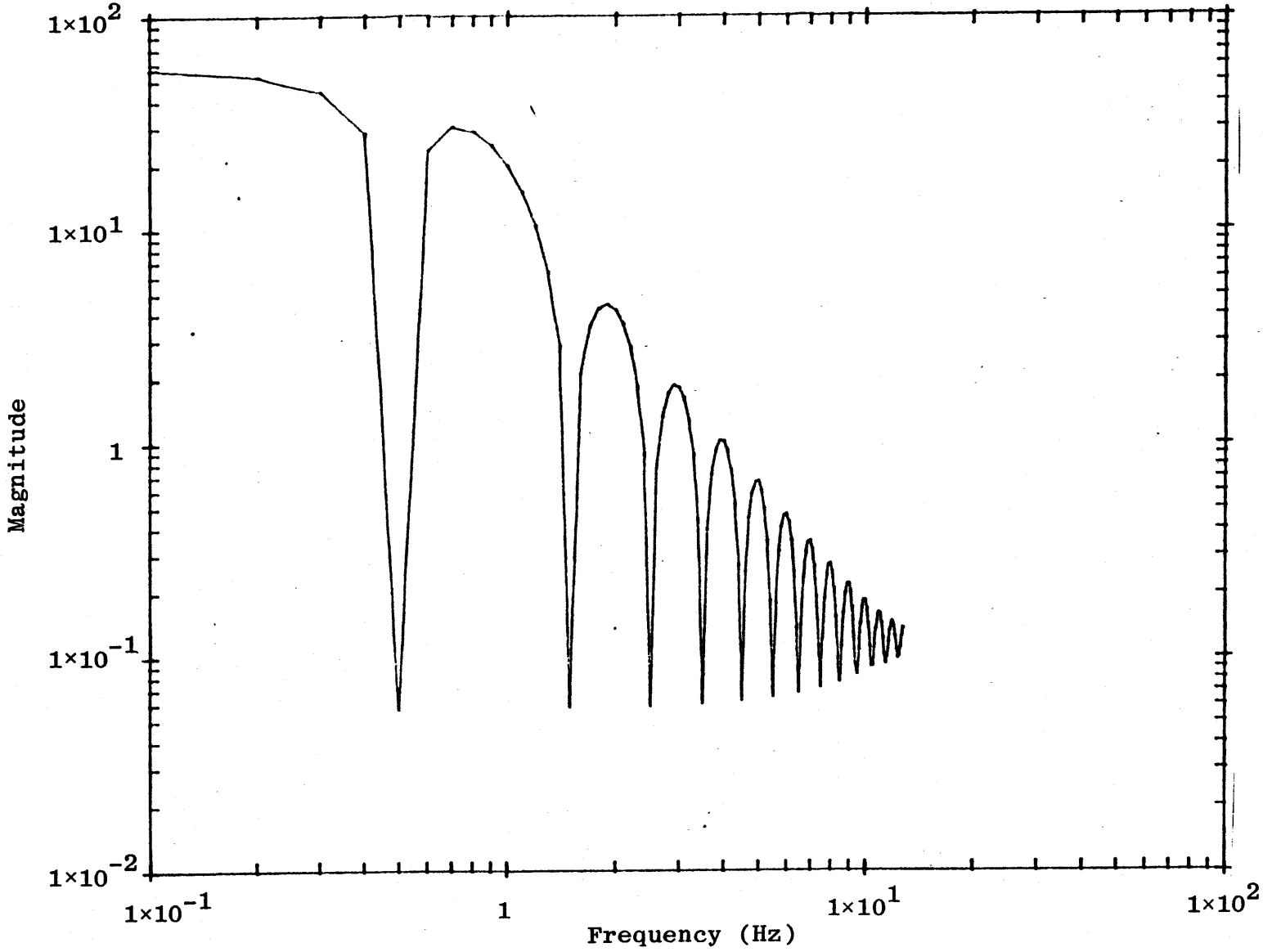

Figure 12. Transform Magnitude, Delayed Damped Sinewaves. D = 1.00

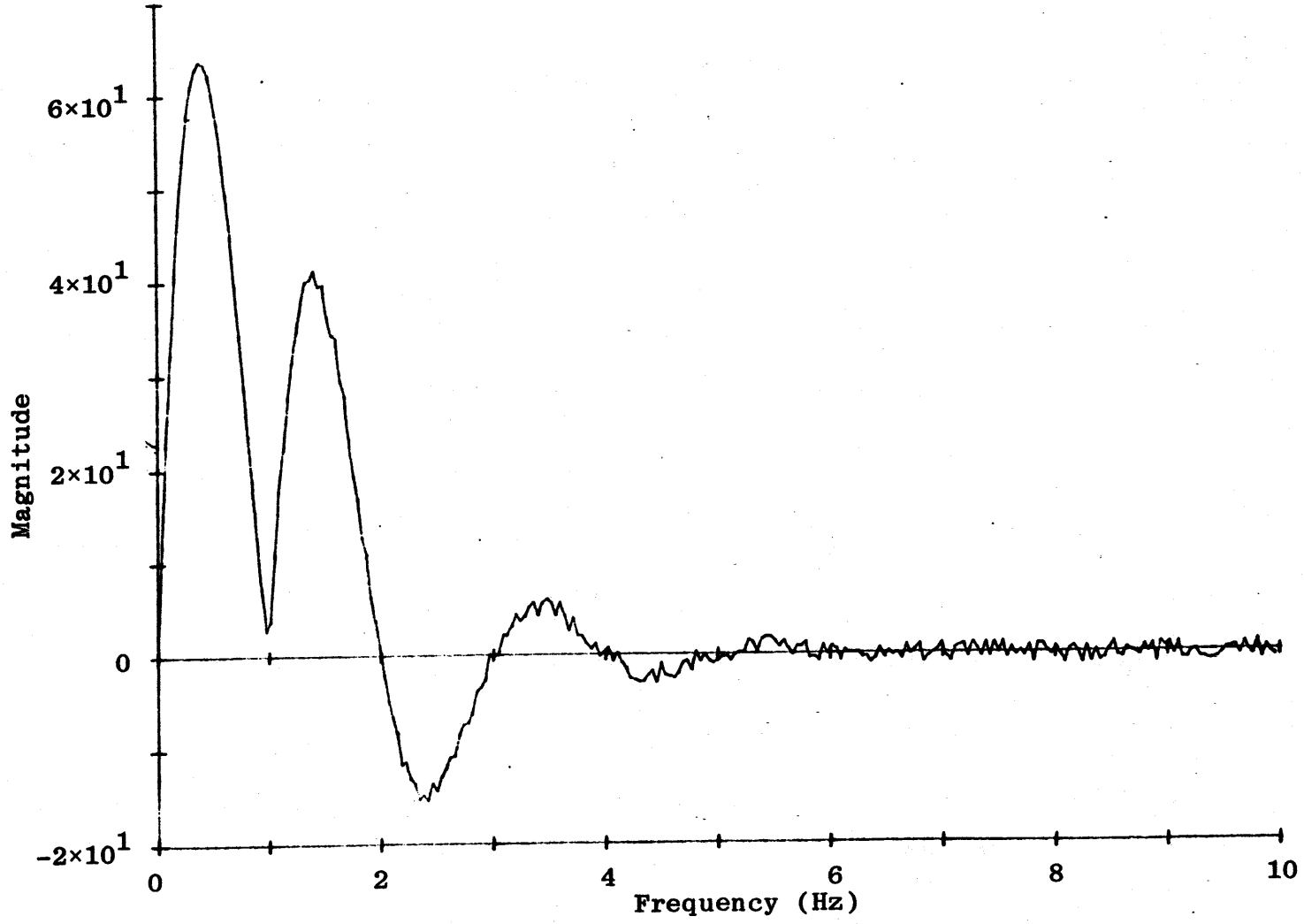

Figure 13. Transform Magnitude, Delayed Damped Sinewaves. D = 1.00, 1% Noise

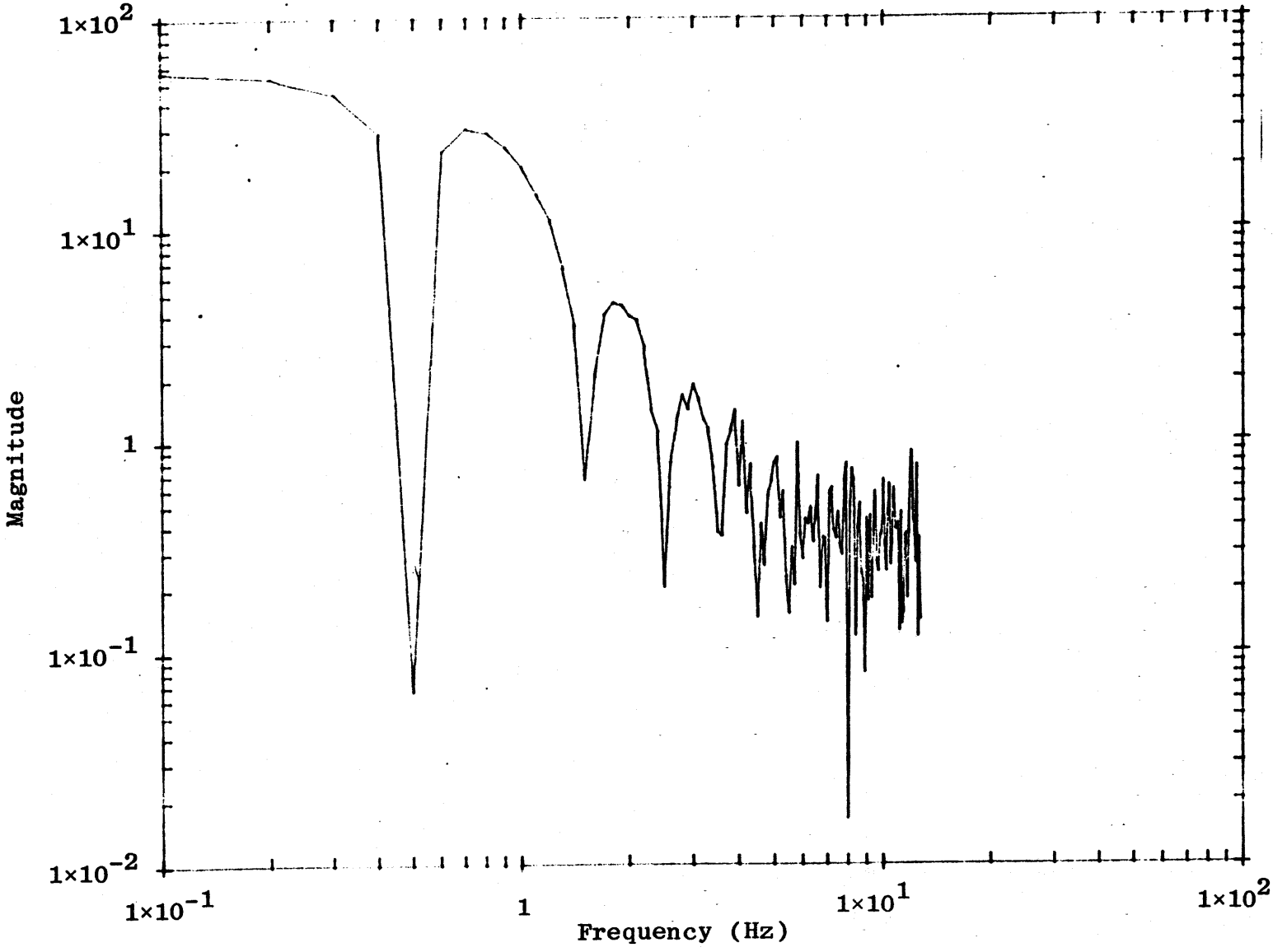

Figure 14. Transform Magnitude, Delayed Damped Sinewaves. D = 1.00, 1% Noise

Table 4. Poles and residues for delay = 1.0.
Prony's method, N = 50, T = .04, 1% noise.

Real Part	Imaginary Part	Real Residue	Imaginary Residue
Order = 25			
S(01) = -.4584541E+00	0.	RESR = .4886385E+00	
S(02) = -.4586901E+00	.6285066E+01	RESR = -.1613987E+00	RESI = -.3695699E-01
S(03) = - 4593837E+00	.1257002E+02	RESR = -.3402992E-01	RESI = -.2945564E-02
S(04) = -.4604932E+00	.1885474E+02	RESR = -.1505037E-01	RESI = -.7700625E-03
S(05) = -.4619509E+00	.2513915E+02	RESR = -.8702552E-02	RESI = -.2929915E-03
S(06) = -.4636677E+00	.3142315E+02	RESR = -.5825886E-02	RESI = -.1335401E-03
S(07) = -.4655377E+00	.3770671E+02	RESR = -.4291344E-02	RESI = -.6719601E-04
S(08) = -.4674443E+00	.4398979E+02	RESR = -.3388019E-02	RESI = -.3572542E-04
S(09) = -.4692674E+00	.5027239E+02	RESR = -.2823705E-02	RESI = -.1950994E-04
S(10) = -.4708910E+00	.5655456E+02	RESR = -.2461044E-02	RESI = -.1069854E-04
S(11) = -.4736229E+00	.7539918E+02	RESR = -.2026719E-02	RESI = -.8251581E-06
S(12) = -.4731418E+00	.6911786E+02	RESR = -.2091442E-02	RESI = -.2776011E-05
S(13) = -.4722110E+00	.6283635E+02	RESR = -.2229566E-02	RESI = -.5723246E-05
Error = .1910876E-14			

Table 5. Poles and residues for delay = 1.0.
Prony's method, N = 50, T = .04, 1% noise.

Real Part	Imaginary Part	Real Residue	Imaginary Residue
Order = 25			
S(01) = -.4543685E+00	0.	RESR = .4890312E+00	
S(02) = -.4332706E+00	.6300913E+01	RESR = -.1585571E+00	RESI = -.3356953E-01
S(03) = -.4332822E+00	.1255303E+02	RESR = -.3433383E-01	RESI = -.2919439E-02
S(04) = -.2593198E+00	.1862412E+02	RESR = -.1149291E-01	RESI = -.3733602E-02
S(05) = -.1358998E+00	.2518019E+02	RESR = -.5542985E-02	RESI = .1480711E-02
S(06) = -.3614176E+00	.3167691E+02	RESR = -.6167102E-02	RESI = .3171212E-02
S(07) = -.6058316E+00	.3726772E+02	RESR = -.6224874E-02	RESI = .2291246E-02
S(08) = -.9040764E+00	.7748416E+02	RESR = -.1728919E-02	RESI = .2506466E-02
S(09) = -.2366074E+00	.6934989E+02	RESR = -.1620911E-02	RESI = .1439478E-02
S(10) = -.9817263E-01	.6258574E+02	RESR = -.9339772E-03	RESI = -.2382959E-03
S(11) = -.6095423E+00	.5562955E+02	RESR = -.9154154E-04	RESI = -.4358939E-02
S(12) = -.1403990E+01	.4946278E+02	RESR = -.8890758E-02	RESI = -.4515599E-02
S(13) = -.1889965E+01	.4464958E+02	RESR = -.8042634E-02	RESI = -.2438708E-02
Error = .5111050E-14			

asynchronism at the ATHAMAS I simulator was at a much higher frequency than the fundamental mode of the cylinder used in the pipe test. The same was true of ground reflection effects when the cylinder was near the ground plane.

It is not difficult to find examples where the delay effect confuses the calculation of object poles. One such example comes from the pipe test with the cylinder at 00-10-30. At this location, the delay is about 47 ns. Figure 15 is the graph of a surface current measurement. Figure 16 is the corresponding Fourier transform magnitude. Poles were calculated from this signal using each of the three methods. The poles vary greatly when the portion of signal analyzed is changed. If the first 40 to 100 ns is analyzed, poles with positive real parts are found. This is reasonable since the signal amplitude is increasing. When 200 ns starting at t = 0 is analyzed, the poles have negative real parts. When more data is added, new pole values are calculated. The location of frequency domain nulls prevents calculation of second and higher order cylinder resonances. The fact that the computed pole values change as the length of signal analyzed is changed causes doubt about the fundamental resonance values. The approach taken in reference 5 was to analyze data over the whole record length. The pole values change little when the data length is close to its maximum value. But it is not possible to conclude that the resulting low frequency pole pair represents the first cylinder natural mode.

The explanation for these difficulties follows from looking at the incident field waveform shown in figure 17.

The delay D = 47 ns produces a peak in the E_x field transform (figure 18) near 10 MHz. In accord with Murphy's law this frequency happens to be quite near the peak in the response transform (figure 16). So this is an example of a peak caused by the ground reflection effect interfering with a response peak. (The graph in figure 17 is for the E_x field at 00-09-30. The cylinder

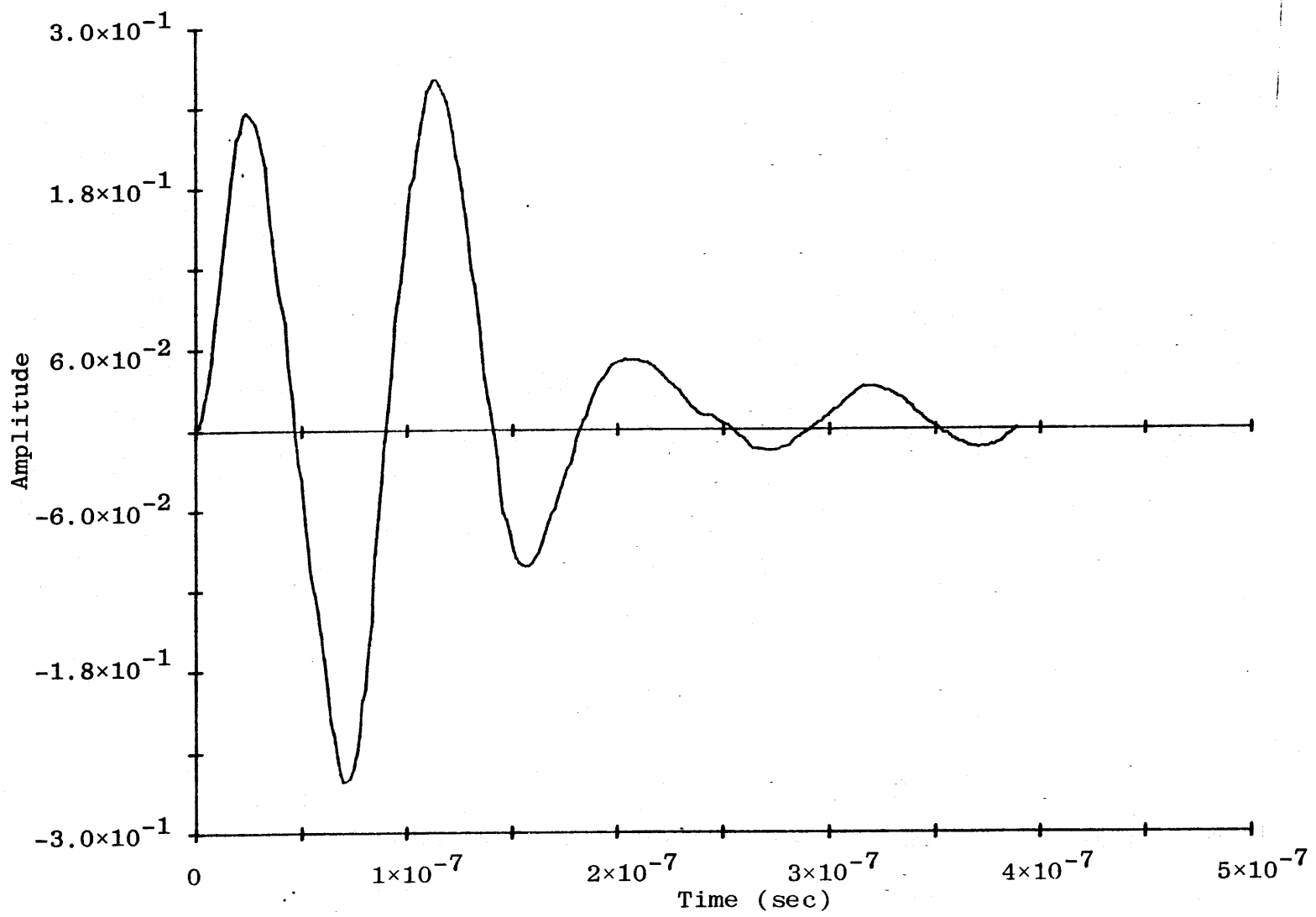

Figure 15. Axial Current Density, Cylinder at 00-10-30 from ATHAMAS I Pipe Test

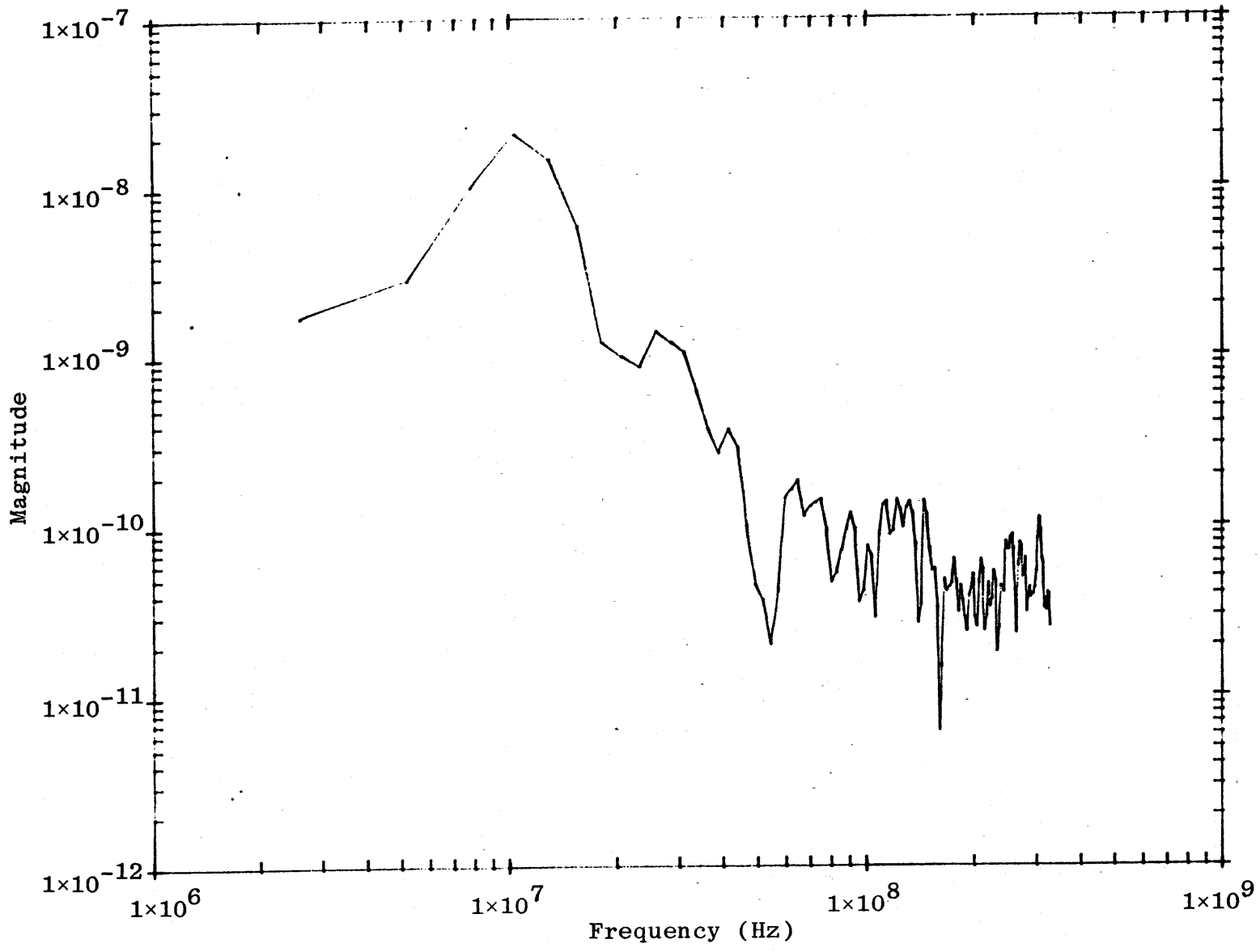

Figure 16. Transform Magnitude of Axial Current Density

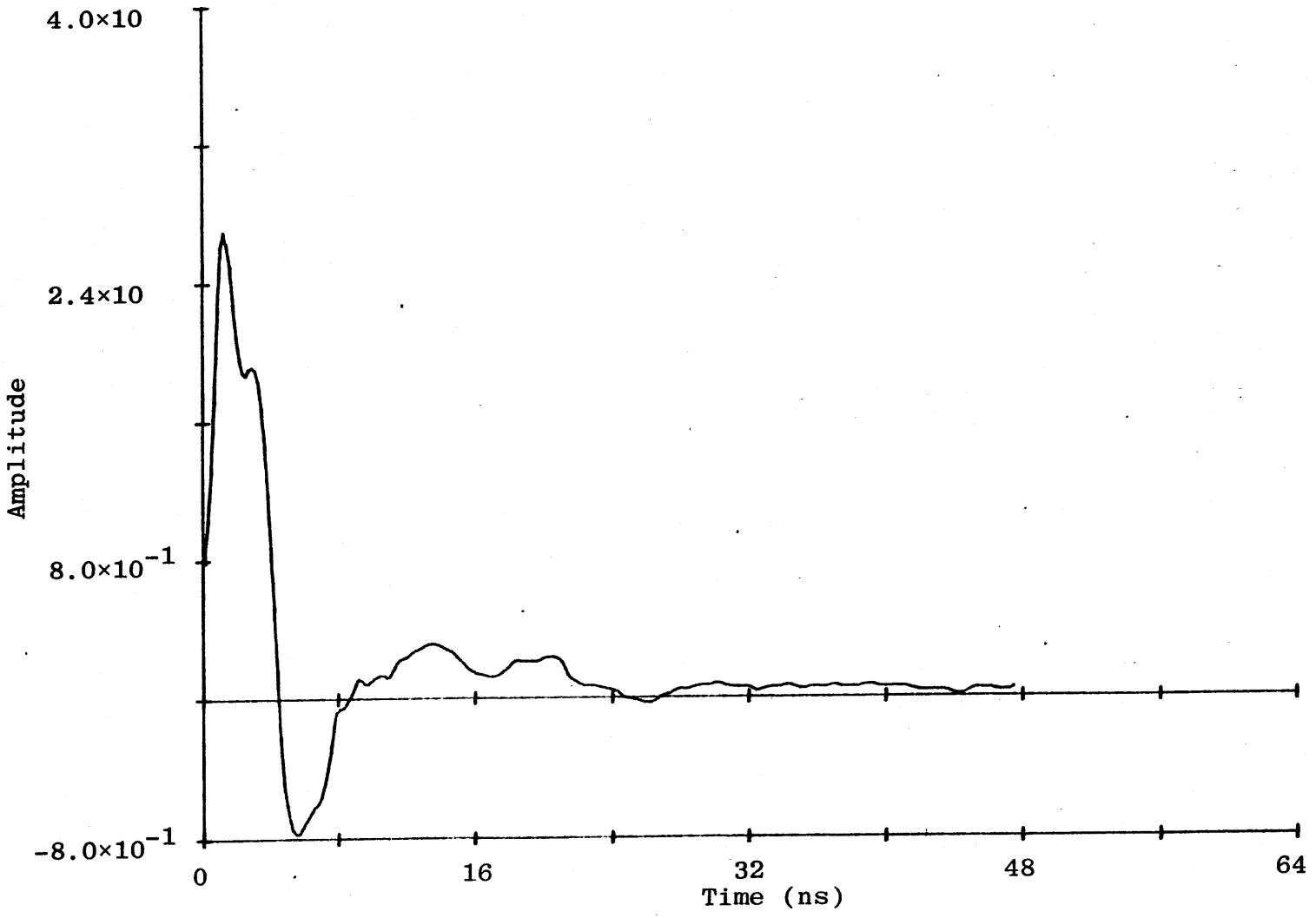

Figure 17. Incident Ex Field at 00-90-30

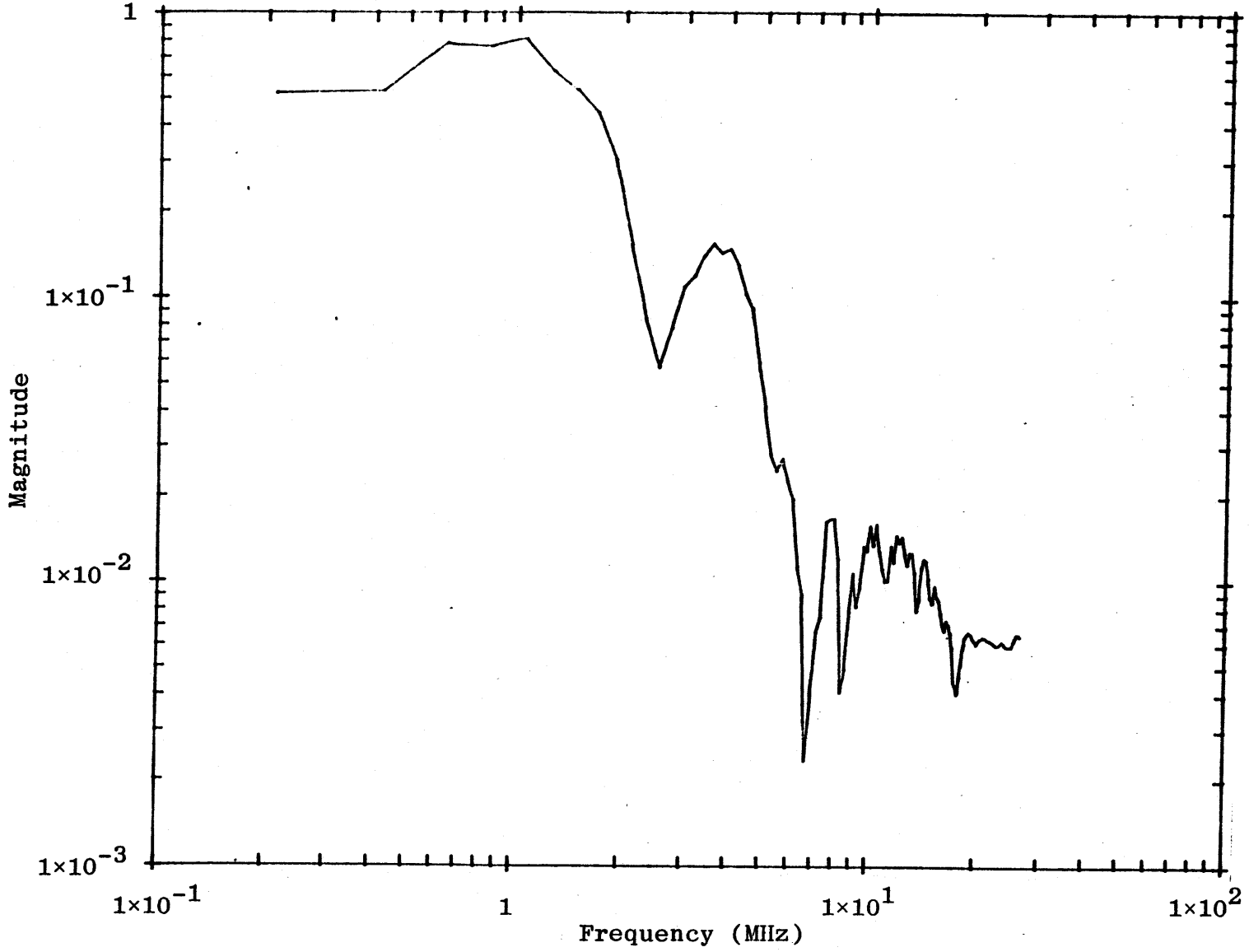

Figure 18. Transform Magnitude of Incident Ex at 00-90-30

was centered at 00-10-30. So the incident field actually seen by the cylinder has a peak even closer to the first cylinder resonance.)

On the basis of equation 4, it would seem reasonable to try to analyze this response data starting from some time after D = 47 ns. This was done. Again each method failed to produce consistent results. The problem here seems to be that the incident field does not stay near zero for times between 47 and 300 ns. In this time range the field doesn't appear to be easily represented by complex exponentials. So its presence interferes with the calculation of response poles. After 300 ns the signal to noise ratio of the response waveform is low and only a small length of record is left. These two factors probably account for the inconsistent results of the pole calculations.

There is a basic problem with trying to approximate the waveform of figure 15 by a sum of complex exponentials. It is simply that this waveform is not a low-order sum of complex exponentials. Equation 3 suggests what should be a better approach. Rewriting equation 3 in a scalar form and allowing for an incident field Laplace transform f(s), the total response can be written as

$$y(s) = f(s)\left[\sum_i \frac{A_i}{s-s_i} + K(s)\, e^{-sD} \sum_i \frac{B_i}{s-s_i}\right] \qquad (5)$$

The A_i and B_i depend on the coupling coefficients, natural mode vectors, and sensor orientation. In the general case $A_i \neq B_i$ and they need to be estimated separately. Equation 5 suggests that the problems with delay and incident field can be overcome by modeling the signal generation process in a way that explicitly separates these components from the object response parameters. This approach will require accurate data on f(s), D, and K(s). Time domain data corresponding to f(s) is available from field map data, D can be calculated from the test configuration, and K(s) can be estimated (see ref. 13).

Section IV

Conclusions

This note is concerned with experimental results. It is necessary to be careful about interpreting the results too generally. For example, it is possible that for some combination of waveform, sampling interval, noise level, etc., one pole calculation technique might be vastly superior to all others. But on the basis of much more experimental evidence than has been shown in the tables, the following conclusions appear to be justified:

(1) For the kind of random noise level expected in EMP testing, Prony's method (using extra poles) works about as well as either of the two iterative methods. The iterative methods are better than Prony's method when the noise level is high.

(2) When the data contains delayed damped sinusoids, poles corresponding to object resonances that are far from delay induced peaks or nulls can be calculated accurately.

(3) The total incident field structure can interfere with or prevent accurate calculation of object parameters. It may be possible to "unravel" the various data components by using information about the incident field, SEM coupling coefficients, and natural modes.

References

1. VanBlaricum, M. L., and R. Mittra, "A Technique for Extracting the Poles and Residues of a System Directly from Its Transient Response," Interaction Note 245, February 1975.

2. Scrivner, G. J., "Prony Analysis in the Presence of Noise," to be published as a Mathematics Note.

3. Sarkar, T. K., J. Nebat, and D. Weiner, "Suboptimal System Approximation/Identification with Known Error," Mathematics Note 49, September 1977.

4. Lager, D. L., H. G. Hudson, and A. J. Poggio, "User's Manual for SEMPEX: A Computer Code for Extracting Complex Exponentials from a Time Waveform," Mathematics Note 45, March 1977.

5. Cordaro, J. T., "Pole Measurements for the ATHAMAS Pipe Test," Mathematics Note 56, August 1977.

6. Baum, C. E., "On the Singularity Expansion Method for the Solution of Electromagnetic Interaction Problems," Interaction Note 88, December 1971.

7. Baum, C. E., "Emerging Technology for Transient and Broad-Band Analysis and Synthesis of Antennas and Scatterers," Proceedings of the IEEE, Vol. 64, No. 11, November 1976. Also, Interaction Note 300, November 1976.

8. Evans, A. G., and R. Fischl, "Optimal Least Squares Time-Domain Synthesis of Recursive Digital Filters," IEEE Trans. on Audio and Electroacoustics, Vol. AU-21, February 1973.

9. Steiglitz, K., and L. E. McBride, "A Technique for the Identification of Linear Systems," IEEE Trans. on Automatic Control, Vol. AC-10, October 1965.

10. Steiglitz, K., "On the Simultaneous Estimation of Poles and Zeros in Speech Analysis," IEEE Trans. on Acoustics, Speech, and Signal Processing, Vol. ASSP-25, June 1977.

11. Hildebrand, F. B., Introduction to Numerical Analysis, McGraw-Hill, 1956.

12. Scott, Larry D., "Deterministic Error Analysis Applied to EMP Simulator Data Acquisition," Measurement Note 24, June 1977.

13. Castillo, J. P., and B. K. Singaraju, "Effects of Wave Reflection on Objects Near a Plane Ground," ATHAMAS Memo 8, May 1975.